Research Article | Vol. 8, No. 11 | 1 Nov 2018 | OPTICAL MATERIALS EXPRESS 3561
Optical Materials EXPRESS

Enhancement of a Cu_2O/ZnO photodetector via surface plasmon resonance induced by Ag nanoparticles

Wei Li,[1] Dengkui Wang,[1,4] Zhenzhong Zhang,[2] Xueying Chu,[3] Xuan Fang,[1] Xinwei Wang,[1] Dan Fang,[1] Fengyuan Lin,[1] Xiaohua Wang,[1] and Zhipeng Wei[1,5]

[1]*State Key Laboratory of High Power Semiconductor Lasers, Changchun University of Science and Technology, 7089 Wei-Xing Road, Changchun 130022, China*
[2]*State Key Laboratory of Luminescence and Applications, Changchun Institute of Optics, Fine Mechanics and Physics, Chinese Academy of Sciences, 3888 Dongnanhu Road, Changchun 130021, China*
[3]*School of Science, Changchun University of Science and Technology, 7089 Wei-Xing Road, Changchun 130022, China*
[4]*wccwss@foxmail.com*
[5]*zpweicust@126.com*

Abstract: The localized surface plasmon resonance enhancement of a Cu_2O photodetector was realized by Ag nanoparticles (NPs) that were fabricated by electrochemical deposition. A ZnO nanowire was used to accelerate carrier separation. An increase of responsivity was achieved based on the coupling interaction between the surface plasmon resonance in the Ag NPs and the Cu_2O film. The photodetector possessed high responsivity (0.27A/W). Compared to the device without Ag NPs, the responsivity was enhanced 20-fold. The excellent comprehensive performance of the Cu_2O/ZnO photodetector reveals that localized surface plasmon resonance is an efficient way to improve the performance of Cu_2O-based photodetectors.

© 2018 Optical Society of America under the terms of the OSA Open Access Publishing Agreement

1. Introduction

Cuprous oxide is a natural p-type direct-gap semiconductor with a 2.1 eV band gap energy [1,2] that can be excited under illumination with the visible light. It is one of the most studied metal oxides for photodetector applications [3,4] because of its high optical absorption coefficient and excellent photoelectric conversion efficiency [5,6]. It is a potential material for applications in electronic and photoelectric devices [7–9]. ZnO plays an important role in the charge separation and migration in the Cu_2O based p-n photodetector [10]. Cu_2O/ZnO heterojunction can provide a larger surface area and more efficient photo-generated electron-hole pair separation. As previously reported [3], a photodetector based on Cu_2O/ZnO heterojunction exhibited responsivity of 8.2 mA W^{-1} in visible light. However, the responsivity of Cu_2O/ZnO photodetectors is inferior in most previous studies because of the low efficiency of the carrier generation. Therefore, it is crucial to find effective ways to improve the performance of Cu_2O-based photodetectors.

Surface plasmon has been widely used to improve the responsivity of photodetectors [11–13]. The localized surface plasmon (LSP) effect of noble metal nanoparticles (NPs) enhance light absorption through coupling between the incident light and metal NPs. The excitation of LSP can be easily achieved in many metal nanoparticles, such as Au, Ag, Al and Pt [14–17]. Ag NPs were widely used in many semiconductors for photoluminescence and absorption enhancement due to their unique features such as relatively low loss, and flexible tenability resonant frequency [18–22]. This is the preferred material for enhancing Cu_2O-based detectors. As previously reported [23], the responsivity of Ag/Cu_2O/ZnO photodetector is 11

#337947 https://doi.org/10.1364/OME.8.003561
Journal © 2018 Received 10 Jul 2018; revised 28 Sep 2018; accepted 28 Sep 2018; published 29 Oct 2018

Optical Materials EXPRESS

times higher than that of a photodetector prepared from pure Cu_2O film, which is still lower than the theoretical expectation.

For this paper, Cu_2O-based photodetectors were fabricated on indium-tin-oxide (ITO) glass substrates via electrochemical deposition following the deposition of ZnO NWs decorated with Ag NPs. A comparative study of Cu_2O photodetectors with and without Ag NPs was performed, to understand the effects of LSP on device performance. It was demonstrated that Ag NPs could greatly increase the responsivity of the photodetector. A tremendous increase in photocurrent (9.4 mA at 2 V bias) was observed for samples with Ag NPs, which was increased 200 times compared to devices without Ag NPs. The photodetector possessed high responsivity (0.27 A/W), which was enhanced 20-fold when compared to the device without Ag NPs. We attributed the improved performance to the effects of LSP on promoting light absorption and the generation and transformation of photon-generated carriers.

2. Experimental detail

The Cu_2O/Ag/ZnO heterostructure was fabricated on an ITO (10 Ω/cm^2) glass substrate. First, ZnO nanowires were prepared by electrochemical deposition. Briefly, a 0.05 mol/L aqueous solution of zinc acetate and hexamethylenetetramine was used as the precursor. ITO glass was used as the cathode to deposit ZnO nanowires at −0.8 V and the deposition was performed at 65 °C for 30 min. Second, Ag NPs were sputtered onto the ZnO NWs to form a Ag/ZnO nanostructure using ion sputtering equipment at room temperature. The current was 2 mA and the sputtering time was 30 s. Finally, Cu_2O film was deposited on Ag/ZnO to form a sandwiched Cu_2O/Ag/ZnO heterostructure. In the typical procedure, an aqueous solution of 0.4 mol/L $CuSO_4$ and 3 mol/L lactic acid was used as the precursor and the pH was adjusted to 10 using NaOH solution. Cu_2O was deposited at 60 °C under −0.6 V for 15 min. To provide ohmic contact, an In electrode was prepared on Cu_2O.

The surface morphology of the metal nanostructures and the Cu_2O/ZnO heterojunction were characterized by scanning electron microscope (SEM, Hitachi S-4800). The crystal structure was studied using an X-ray diffractometer (XRD, Bruker D8 Focus). The absorption spectrum was measured by a UV-visible spectrophotometer (UV-2450) and the current-voltage (I-V) curves of the heterojunction devices and ohmic contact characteristic curve were measured using a source meter unit (Keithley 2400) at different bias voltages and the photoresponse properties of the photodetectors were characterized using a 150 W Xe lamp as the excitation source.

3. Results and discussion

The X-ray diffraction spectrum of Cu_2O/ZnO is shown in Fig. 1(a). Several strong diffraction peaks that correspond to the cubic phase of Cu_2O (JCPDS 65-3288) are identified as the (110), (111), (200) and (220) face. The diffraction peaks of the ZnO and ITO substrate are relatively weak due to their coverage with a thick Cu_2O film. The peak located at 34.4° could be indexed to the (002) face of ZnO. The ZnO NWs have a c-axis preferred orientation and the insets of Fig. 1(a) are SEM images of the Cu_2O/ZnO NWs heterojunction at the top and side view. The Cu_2O films consist of a cubic structure that compacts well together. Cross-section images show that the thickness of the Cu_2O film is about 4.3μm and the ZnO NWs array is immersed in Cu_2O film. It can be observed that the Cu_2O filled well in the space between ZnO nanowires under the present processing conditions, which is expected to increase the contact area of the heterojunction effectively and greatly enhance the concentration of electron-hole pairs. The UV-visible absorption spectra of Cu_2O/ZnO were measured, as shown in Fig. 1(b). The absorption edges located in the ultraviolet and visible light range are obviously observed, which come from the absorption of ZnO NWs and Cu_2O film, respectively [24]. The inset of Fig. 1(b) is the plot of $(\alpha h\upsilon)^2$ vs. $h\upsilon$ for the Cu_2O/ZnO. The band gap values are calculated according to:

Optical Materials EXPRESS

$$\alpha h\nu = \left(h\nu - E_g\right)^{\frac{1}{2}} \quad (1)$$

where α is the absorption coefficient; h is the Planck constant, and Eg is the band gap of the semiconductor. The band gap energies are determined to be 2.16 eV and 3.30 eV from the UV-visible absorption spectrum, which are accordance with the band gap of Cu_2O and ZnO.

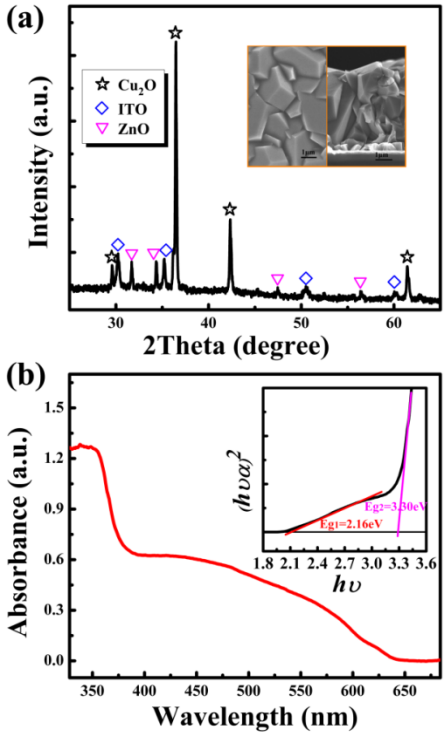

Fig. 1. (a) The corresponding XRD patterns of Cu_2O/ZnO; the inset is the SEM images of Cu_2O/ZnO on ITO with the top and cross-section, respectively. (b) The UV-visible spectra of Cu_2O/ZnO, the inset is the plot of $(\alpha h\upsilon)^2$ vs. $h\upsilon$ for the Cu_2O/ZnO films.

As is well known, the good energy match between light absorption and LSP is the key factor to achieving enormous response enhancement. The spectral shape and position of the localized surface plasmon resonances (LSPR) in the metal nanoparticles are highly sensitive to size, and internal gap [25–28]. Finite difference time domain (FDTD) simulations were carried out to determine the size of Ag NPs and ensure that the resonance peaks could match the absorption edges of Cu_2O. The extinction spectra of Ag NPs are shown in Fig. 2(a). The interspace gap (g) between two NPs was 10 nm, and the range of the radius is 45-65 nm. The LSPR spectrum exhibits clearly observable peaks in the ultraviolet and visible light range for the Ag NPs. The peaks around ultraviolet are related multipole resonance. The visible resonance peaks have significantly red-shifted when the size of Ag NPs increased. The extinction peak shifts from 508 nm to 671 nm when the radius of the Ag NPs increases from 45 nm to 65 nm; in addition, the resonance intensity becomes stronger when the size of the Ag NPs increases. It is found that when the radius of the Ag NPs is 55 nm, the maximum resonance intensity locates at 570-610 nm, which favorably matches with the Cu_2O absorption edge.

To further investigate the enhancement of responsivity introduced by the LSPR of Ag NPs, we have prepared Ag NPs at the Cu_2O/ZnO interface. Figure 2(b) shows the UV-visible spectra of Cu_2O/ZnO and Cu_2O/Ag/ZnO. The inset in Fig. 2(b) is SEM images of Ag NPs

Optical Materials EXPRESS

sputtering for 30 s. Ag NPs of approximate size 110 nm were randomly distributed. Compared to the sample without Ag NPs, the LSPR effect of Ag nanoparticles enhanced the light absorption, through light coupling efficiency by matching the resonance frequency and wavelengths. The specific wavelength would be coupled with the surface plasmon in Ag nanoparticles. The absorption at specific wavelength will be enhanced, thus, how the LSPR enhanced absorption for the specific wavelength of coupled light can be determined.

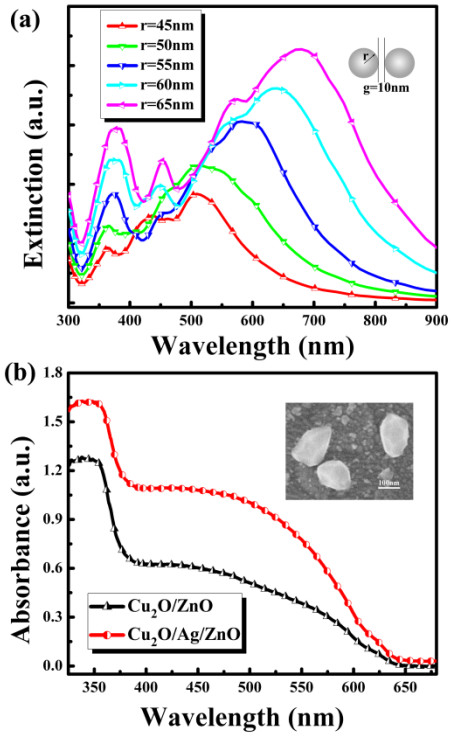

Fig. 2. (a) Extinction spectra of Ag NPs, (b) The absorption spectra of Cu_2O/ZnO films with and without Ag NPs, the inset is SEM images of Ag NPs.

In order to understand the effects of Ag NPs, we performed wavelength-dependent responsivity tests. The photo and dark current-voltage characterization were carried out for the Cu_2O/ZnO and Cu_2O/Ag/ZnO heterostructure, as shown in Fig. 3(a). Insert of Fig. 3(a) is the I-V curve between two In electrodes on Cu_2O, which implies that the contact between In electrode and Cu_2O is ohmic. The responsivity spectra of Cu_2O/ZnO and Cu_2O/ZnO at 2V bias are shown in Fig. 3(b) and the photo-current obtained from Cu_2O/ZnO is $4.6*10^{-5}$ A. However, a tremendous increase of photocurrents is observed for samples with Ag NPs. The photocurrent of Cu_2O/Ag/ZnO is $9.4*10^{-3}$ A at 2V bias, which is increased 200-fold. For the I-V characterization, both devices exhibit small dark-current. The dark current of Cu_2O/Ag/ZnO has slightly increased, which is attributed to the interface modification by Ag NPs. this indicates that Ag NPs play an important role on enhancing the photocurrent. Figure 3(b) shows the responsivity of Cu_2O/ZnO and Cu_2O/Ag/ZnO under Xe lamp illumination at wavelengths in the range 300-700 nm. It is found that the responsivity of Cu_2O/Ag/ZnO is greater than that of Cu_2O/ZnO in the whole range, particularly at 564 nm near the LSP of Ag NPs. Notably; the peak responsivity value had increased from 0.013 A/W to 0.27 A/W. Two factors influenced the response of photodetector. First, the increased intensities of electric fields resulted in increased light absorption because the optical transition rate was proportional to the square of the electric field amplitude [28]. Second, the absorption

Optical Materials EXPRESS

efficiency of photodetector increased in the visible light range because of the LSPR coupling effect of Ag NPs.

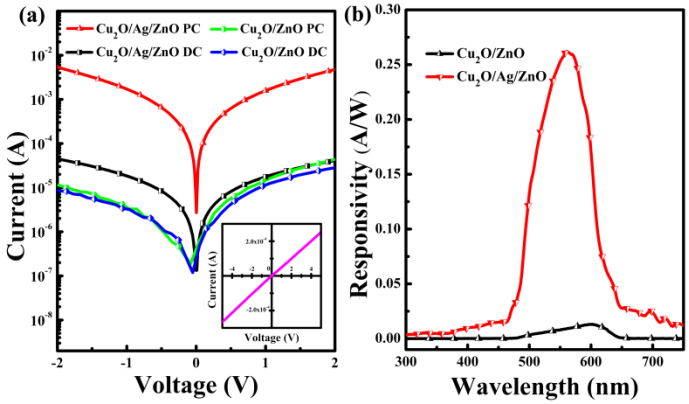

Fig. 3. (a) I-V characteristics of the Cu_2O/ZnO and Cu_2O/Ag/ZnO photodetector, the insert is current-voltage curve between two In electrode on Cu_2O. (b) Spectral response of the Cu_2O/ZnO and Cu_2O/Ag/ZnO photodetector at 2V bias.

Figure 4(a) and (b) are the photo-response spectra of Cu_2O/ZnO and Cu_2O/Ag/ZnO photodetectors for 0.1-V bias. The peak responsivities are 0.013 A/W (2 V) for Cu_2O/ZnO photodetectors and 0.27 A/W (2 V) for Cu_2O/Ag/ZnO photodetectors. The LSPR absorption peak of the Ag NPs shows a 40 nm blue shift (from 604 to 564 nm) which is caused by the resonant wavelength offset of the Ag NPs, due to the large size distribution of the Ag particles. Figure 4(c) shows the peak responsivity as a function of the bias voltage. The linear relationship can be observed from 0.1 to 2 V for two devices, which indicate no carrier mobility saturation or sweep-out effect [29]. It is clear that the responsivity of the photodetector with Ag NPs reveals a remarkable increase with applied voltages, which is due to the LSPR coupling absorption enhancement. Besides the responsivity, detectivity is another important parameter that reflects the photodetector sensitivity to incident light. The major noise in our devices should be the thermal noise and shot noise, thus the detectivity (D^*) can be estimated via the following equation [29]:

$$D^* = \frac{A^{1/2} R}{\left(4k_0 T / R_{dark} + 2qI_{dark}\right)^{1/2}} \tag{2}$$

where A is the active area, R is the responsivity, k_0 is the Boltzmann constant, T is the temperature, R_{dark} is the equivalent resistance at the bias point, q is the elementary charge, and I_{dark} is the dark current at the bias point and the function between detectivity and bias voltage was shown in Fig. 4(d). The maximum detectivity of Cu_2O/Ag/ZnO photodetectors was $3.3*10^{10}$ Jones, which was increased 37-fold compared to Cu_2O/ZnO photodetectors ($8.9*10^8$ Jones). The large detectivity of Cu_2O/Ag/ZnO photodetectors was attributed to the low dark current and high responsivity.

Optical Materials EXPRESS

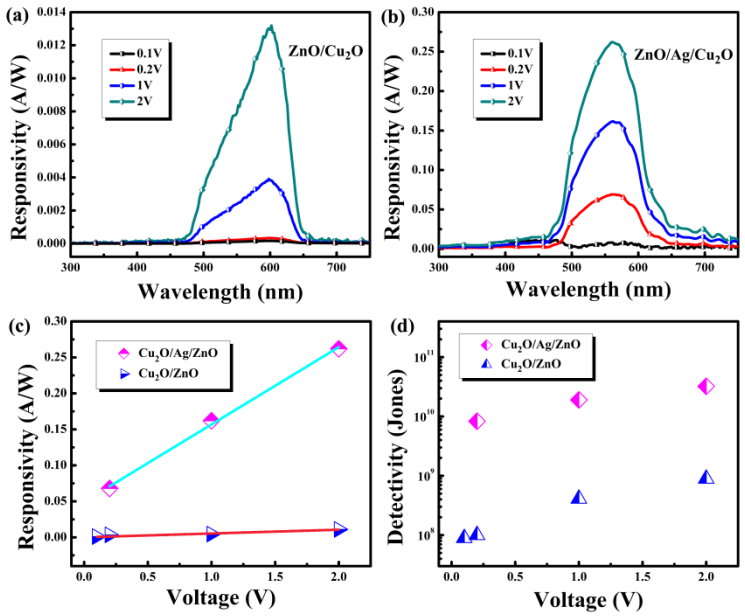

Fig. 4. Spectral response of (a) Cu_2O/ZnO and (b) Cu_2O/Ag/ZnO photodetectors, (c) Peak responsivity and (d) Detectivity of Cu_2O/ZnO and Cu_2O/Ag/ZnO photodetectors as a function of the bias voltage.

4. Conclusion

In summary, a significant responsivity enhancement for the Cu_2O/Ag/ZnO photodetector has been realized for the surface plasmon resonance of Ag nanoparticles. The I-V and responsivity measurements indicate that the sample decorated with Ag NPs exhibits high photocurrent ($9.4*10^{-3}$A) and responsivity (0.27 A/W), with 200-fold and 20 fold enhancement compared to Cu_2O/ZnO photodetectors, respectively. This photodetector has excellent comprehensive performance, such as a high photocurrent, high responsivity and large detectivity. Due to the great enhancement of the Ag surface plasmon, Cu_2O/Ag/ZnO photodetectors should have potential applications in image sensors.

Funding

National Natural Science Foundation of China (61704011, 61674021, 11674038, 61574022, 61474010); the Developing Project of Science and Technology of Jilin Province (20170520118JH, 20160519007JH, 20160520117JH, 20160204074GX); the Innovation Foundation of Changchun University of Science and Technology (XJJLG-2016-11, XJJLG-2016-14).

References

1. H. Makhlouf, O. Messaoudi, A. Souissi, I. Ben Assaker, M. Oueslati, M. Bechelany, and R. Chtourou, "Tuning of Ag doped core-shell ZnO NWs/Cu_2O grown by electrochemical deposition," Mater. Res. Express **2**(9), 095002 (2015).
2. H. Tanaka, T. Shimakawa, T. Miyata, H. Sato, and T. Minami, "Effect of AZO film deposition conditions on the photovoltaic properties of AZO-Cu_2O heterojunctions," Appl. Surf. Sci. **244**(1–4), 568–572 (2005).
3. Z. Bai and Y. Zhang, "Self-powered UV-visible photodetectors based on ZnO/Cu_2O nanowire/electrolyte heterojunctions," J. Alloys Compd. **675**, 325–330 (2016).
4. N. G. Elfadill, M. R. Hashim, K. M. A. Saron, K. Chahrour, M. A. Qaeed, and M. Bououdina, "Ultraviolet-Visible photo-response of p-Cu_2O/n-ZnO heterojunction prepared on flexible (PET) substrate," Mater. Chem. Phys. **156**, 54–60 (2015).

Optical Materials EXPRESS

5. L. Liao, B. Yan, Y. F. Hao, G. Z. Xing, J. P. Liu, B. C. Zhao, Z. X. Shen, T. Wu, L. Wang, J. T. L. Thong, C. M. Li, W. Huang, and T. Yu, "P-type electrical, photoconductive, and anomalous ferromagnetic properties of Cu_2O nanowires," Appl. Phys. Lett. **94**(11), 113106 (2009).
6. Y. Hou, X. Y. Li, Q. D. Zhao, X. Quan, and G. H. Chen, "Fabrication of Cu_2O/TiO_2 nanotube heterojunction arrays and investigation of its photoelectrochemical behavior," Appl. Phys. Lett. **95**(9), 093108 (2009).
7. C. M. McShane, W. P. Siripala, and K. S. Choi, "Effect of junction morphology on the performance of polycrystalline Cu_2O homojunction solar cells," J. Phys. Chem. Lett. **1**(18), 2666–2670 (2010).
8. P. Poizot, S. Laruelle, S. Grugeon, L. Dupont, and J. M. Tarascon, "Nano-sized transition-metal oxides as negative-electrode materials for lithium-ion batteries," Nature **407**(6803), 496–499 (2000).
9. K. Matsuzaki, K. Nomura, H. Yanagi, T. Kamiya, M. Hirano, and H. Hosono, "Epitaxial growth of high mobility Cu2O thin films and application to p-channel thin film transistor," Appl. Phys. Lett. **93**(20), 202107 (2008).
10. K. P. Musselman, A. Wisnet, D. C. Iza, H. C. Hesse, C. Scheu, J. L. MacManus-Driscoll, and L. Schmidt-Mende, "Strong efficiency improvements in ultra-low-cost inorganic nanowire solar cells," Adv. Mater. **22**(35), E254–E258 (2010).
11. R. Jia, G. Lin, D. Zhao, Q. Zhang, X. Y. Lin, N. K. Gao, and D. Liu, "Sandwich-structured Cu_2O photodetectors enhanced by localized surface plasmon resonances," Appl. Surf. Sci. **332**, 340–345 (2015).
12. G. Kaur, K. L. Yadav, and A. Mitra, "Localized surface plasmon induced enhancement of electron-hole generation with silver metal island at n-Al:ZnO/p-Cu_2O heterojunction," Appl. Phys. Lett. **107**(5), 053901 (2015).
13. J. K. Sheu, M. L. Lee, and Y. C. Lin, "Surface Plasmon-Enhanced GaN Metal-Insulator-Semiconductor Ultraviolet detectors with Ag nanoislands embedded in a silicon dioxide gate layer," IEEE. J. Sel. Top. Quant. **20**(6), 137–141 (2014).
14. Z. H. Chen, Y. B. Tang, C. P. Liu, Y. H. Leung, G. D. Yuan, L. M. Chen, Y. Q. Wang, I. Bello, J. A. Zapien, W. J. Zhang, C. S. Lee, and S. T. Lee, "Vertically Aligned ZnO Nanorod Arrays Sentisized with Gold Nanoparticles for Schottky Barrier Photovoltaic Cells," J. Phys. Chem. C **113**(30), 13433–13437 (2009).
15. M. K. Krug, M. Reisecker, A. Hohenau, H. Ditlbacher, A. Trugler, U. Hohenester, and J. R. Krenn, "Probing plasmonic breathing modes optically," Appl. Phys. Lett. **105**(17), 171103 (2014).
16. S. Butun, N. A. Cinel, and E. Ozbay, "LSPR enhanced MSM UV photodetectors," Nanotechnology **23**(44), 444010 (2012).
17. Z. Guo, D. Jiang, M. Zhao, F. Guo, J. N. Pei, R. S. Liu, L. Sun, N. Hu, and G. Y. Zhang, "Surface plasmon enhanced the responsivity of the ZnO/Pt nanoparticles/ZnO sandwich structured photodetector via optimizing the thickness of the top ZnO layer," Solid-State Electron. **124**, 24–27 (2016).
18. M. Pirhashemi and A. Habibi-Yangjeh, "Ultrasonic-assisted preparation of plasmonic ZnO/Ag/Ag_2WO_4 nanocomposites with high visible-light photocatalytic performance for degradation of organic pollutants," J. Colloid Interface Sci. **491**, 216–229 (2017).
19. G. Lin, Q. Zhang, X. Lin, D. F. Zhao, R. Jia, N. K. Gao, Z. Y. Zuo, X. G. Xu, and D. Liu, "Enhanced photoluminescence of gallium phosphide by surface plasmon resonances of metallic nanoparticles," RSC Advances **5**(60), 48275–48280 (2015).
20. S. C. Zhu, Z. G. Yu, L. X. Zhao, J. X. Wang, and J. M. Li, "Enhancement of the modulation bandwidth for GaN-based light-emitting diode by surface plasmons," Opt. Express **23**(11), 13752–13760 (2015).
21. S. J. Park, H. H. Sohee-Jeong, H. H. Park, S. W. Lee, S. Jeon, J. H. Lee, D. G. Choi, J. H. Jeong, and J. H. Choi, "Optimized film processing of nanosilver colloids for photoluminescence enhancement," J. Nanosci. Nanotechnol. **11**(1), 422–426 (2011).
22. S. Ren, G. Zhao, Y. Wang, B. Wang, and Q. Wang, "Enhanced photocatalytic performance of sandwiched ZnO@Ag@Cu_2O nanorod films: the distinct role of Ag NPs in the visible light and UV region," Nanotechnology **26**(12), 125403 (2015).
23. Y. Liu, F. Ren, S. Shen, Y. M. Fu, C. Chen, C. Liu, Z. Xing, D. Liu, X. H. Xiao, W. Wu, X. D. Zheng, Y. C. Liu, and C. Z. Jiang, "Efficient enhancement of hydrogen production by Ag/Cu2O/ZnO tandem triple-junction photoelectrochemical cell," Appl. Phys. Lett. **106**(12), 123901 (2015).
24. J. Li, H. Li, Y. Xue, H. Fang, and W. Wang, "Facile electrodeposition of environment-friendly Cu_2O/ZnO heterojunction for robust photoelectrochemical biosensing," Sensor. Actuat. Biol. Chem. **191**(2), 619–624 (2014).
25. Z. J. Yang, Z. S. Zhang, L. H. Zhang, Q. Q. Li, Z. H. Hao, and Q. Q. Wang, "Fano resonances in dipole-quadrupole plasmon coupling nanorod dimers," Opt. Lett. **36**(9), 1542–1544 (2011).
26. E. Prodan, C. Radloff, N. J. Halas, and P. Nordlander, "A hybridization model for the plasmon response of complex nanostructures," Science **302**(5644), 419–422 (2003).
27. J. Ye, F. Wen, H. Sobhani, J. B. Lassiter, P. Van Dorpe, P. Nordlander, and N. J. Halas, "Plasmonic Nanoclusters: Near Field Properties of the Fano Resonance Interrogated with SERS," Nano Lett. **12**(3), 1660–1667 (2012).
28. D. M. Schaadt, B. Feng, and E. T. Yu, "Enhanced semiconductor optical absorption via surface plasmon excitation in metal nanoparticles," Appl. Phys. Lett. **86**(6), 063106 (2005).
29. D. Jiang, C. Tian, G. Yang, J. M. Qin, Q. C. Liang, J. X. Zhao, J. H. Hou, and S. Gao, "$Mg_xZn_{1-x}O$ solar-blind photodetectors fabricated by RF magnetron sputtering with combinatorial targets," Mater. Res. Bull. **67**, 158–161 (2015).

159.226.165.17 {ts '2019-08-11 22:44:20'}